S09

Proceedings of the 5th International Conference on Inverse Problems in Engineering: Theory and Practice, Cambridge, UK, 11-15th July 2005

DRAPE OPTIMISATION IN WOVEN COMPOSITE MANUFACTURING

A. A. SKORDOS[1], C. MONROY ACEVES[2] and M. P. F. SUTCLIFFE[3]
Department of Engineering, University of Cambridge, Trumpington Street, Cambridge, CB1 2PZ, UK
e-mail: [1]aas46@cam.ac.uk; [2]cm352@cam.ac.uk; [3]mpfs@eng.cam.ac.uk

Abstract – This paper addresses the optimisation of forming in manufacturing of composites. A simplified finite element model of draping is developed and implemented. The model incorporates the non-linear shear response of textiles and wrinkling due to buckling of tows. The model is validated against experimental results and it is concluded that it reproduces successfully the most important features of the process. The simple character of the model results in low computational times that allow its use within an optimisation procedure. A genetic algorithm is used to solve the optimisation problem of minimising the wrinkling in the formed component by selecting a suitable holding force distribution. The effect of regularisation is investigated and the L-curve is used to select a regularisation parameter value. Optimised designs resulting from the inversion procedure have significantly lower wrinkling than uniform holding force profiles, while regularisation allows force gradients to be kept relatively low so that suggested process designs are feasible.

1. INTRODUCTION

The manufacturing of woven reinforcement polymer composites involves a forming or draping stage during which the reinforcement fabric is placed around the manufacturing tool, a consolidation or impregnation stage during which the polymer matrix permeates the reinforcement and, in the case of thermosetting matrices, a cure stage during which the cross-linking reaction transforms the liquid polymeric matrix to a solid glass. The stage of fabric draping affects the final quality of the produced component in a number of ways. The orientation of fibre tows which is defined by the fabric-tool interaction during draping determines the local mechanical properties of the finished part as well as the permeability and the thermal conductivity. While variations of the stiffness tensor over the produced component are a very important design parameter, variations of permeability and thermal conductivity determine the feasibility of manufacturing a component. For instance, excessive fabric shear can decrease the local permeability of reinforcement resulting in the formation of dry spots during impregnation. Similarly, low fibre volume fraction causes the formation of a low conductivity polymer-rich region which can undergo detrimental temperature overshoots during the cure stage. Furthermore, wrinkles or creases can form during draping that render the finished component unacceptable to the end user.

Models that simulate draping are divided into two main categories. Kinematic models [1, 15, 18, 19] perform mapping of the reinforcement to the manufacturing tool. In those models, fibre tows are inextensible and rotate freely at the crossover points. As a result, pure shear is the only active deformation mechanism. This approach is simple to implement and provides very fast solutions. However, kinematic modelling is a purely geometric approach and does not take into account the mechanics of draping. As a consequence effects related to the mechanical response of the fabric, e.g. wrinkling, cannot be reproduced. The second category of models includes efforts based on the use of finite elements [2, 3, 14]. In these models, which are usually implemented in a explicit formulation, the fabric is represented by an assembly of shell elements in contact with the rigid tool surface, while both material and geometric non-linearities are taken into account. Finite element models reproduce successfully mechanical effects with the disadvantage of very high computational cost. When the objective of drape modelling is its use within a process design and optimisation procedure computational cost becomes a significant issue and shell-based finite element models become very expensive. In contrast, kinematic models can be used when the objectives of optimisation relate only to geometric effects, such as shear angle distribution or final shape. An intermediate modelling methodology which combines simplicity with the incorporation of mechanical effects was presented in [16]. This simplified finite element model simulates the woven material as a truss comprising stiff elastic members which are arranged in a lattice and represent the tows, and plastic diagonal members that incorporate the strain dependent shear behaviour of the reinforcement. This methodology is appropriate for use within an optimisation procedure as solution times are relatively low and the most important effects can be reproduced successfully.

Efforts on computational optimisation of composites manufacturing have been focused on the impregnation and cure stages. Optimisation of the filling stage of liquid composite moulding with respect to the

location of injection and outlet ports has been performed using cascade optimisation [4] and evolutionary algorithms [8, 18]. Research on optimisation of the curing stage has addressed the problem of selection of cost-effective thermal profiles using genetic algorithms [10, 17] and specification of tool geometries that compensate for manufacturing distortion [21].

The present paper addresses the optimisation of the holding force distribution around the edge of the manufacturing tool during forming, with the objective of minimising wrinkling. The simplified finite element model presented in [16] is extended in order to include wrinkling of the woven material resulting from buckling of tows, based on the concepts developed for the modelling of membrane wrinkling [11]. The combined model is implemented in a finite element code and evaluated against experimental results obtained from forming of a hemisphere. The sensitivity of wrinkling strain to the holding force distribution is investigated. An inverse scheme based on genetic algorithms is presented for the solution of the optimisation problem. The effect of regularisation, which is used to damp out unrealistically high holding force gradients, is also investigated.

2. DRAPING MODEL

2.1 Model description

The draping model represents the woven fabric as an assembly of bars, as shown in Figure 1.a. All bars are connected at the corners of the unit cell of the model (Figure 1.b) via pin joints. The sides of the unit cell represent the tows of the textile and the diagonal bars govern the non-linear shear behaviour of the assembly. This arrangement allows the trellising action observed in practice to be reproduced when the effective stiffness of the tow bars is significantly higher than the stiffness of the diagonal bars. It should be noted that the size of the unit cell is greater than the actual size of the textile unit cell.

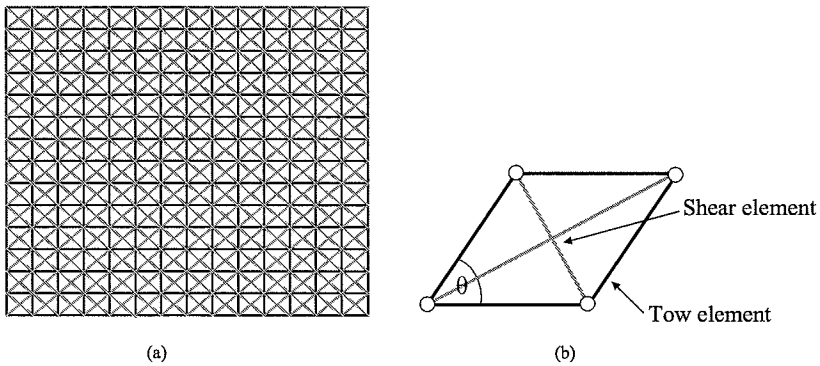

Figure 1. Truss model of a woven fabric.

The solution of the truss model is performed using a finite element code that can accommodate geometric and material non-linearities. Tow elements are considered elastic in tension. The incorporation of wrinkling is based on a activation/deactivation strategy applied to tow elements. Deactivation is triggered by the existence of finite compressive strain in the element. A check is performed at the end of each increment of the finite element analysis. If the strain of an element is below a pre-specified threshold the element is removed from subsequent steps. The non-linear stress-strain response of the shear element is simulated by a strain dependent plastic material model. The strain in the finite element implementation of the model follows the Green-Lagrange definition. Under the assumption that tow strain is low, the cell angle is related to Green-Lagrange strain as follows:

$$\varepsilon_{major} = \cos^2\left(\theta/2\right) - 0.5 \tag{1}$$

$$\varepsilon_{minor} = \sin^2\left(\theta/2\right) - 0.5 \tag{2}$$

where ε_{major} is the strain of the major diagonal, ε_{minor} the strain of the minor diagonal and θ the unit cell angle. Thus, the response of the two diagonals is symmetric and each of them carries half of the shear stress acting on the unit cell.

The shear response of woven textiles is obtained using picture frame and bias extension tests. The shearing behaviour can be divided into two distinct regions [7, 13]. Before fabric lock-up, where low loads are required to shear the material; and after lock up, where a steep increase in the load occurs. Fabric lock-up occurs when high angles of tow rotation result in the development of significant compressive

forces between crossing tows. The following relationship for the slope of the stress-strain curve is used to model this behaviour:

$$S = (S_\infty - S_o)\,(N\,(\mu, \sigma, |\varepsilon|) - 1) + S_\infty \tag{3}$$

Here S is the slope of the stress-strain curve, S_o and S_∞ are the values of the slope at low and high strains, respectively. N denotes the normal distribution function with mean μ and standard deviation σ, which is used to express the transition from low to high shear modulus typically observed. Figure 2 illustrates a typical stress-strain curve produced using eqn.(3). The response is divided into the two regions observed in experiments, one corresponding to low strain and one to high strain. The transition occurs at strain μ and has breadth equal to 4σ.

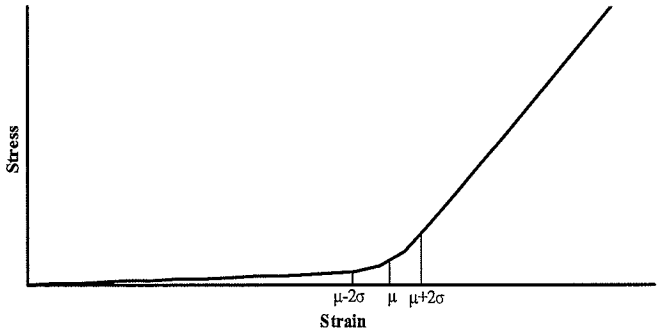

Figure 2. Response of shear elements using equation eqn.(3).

The action of the blank holder on the woven material is incorporated in the model by including a group of bar elements connected to the nodes of the model in contact with the blank holder. These elements are fixed with respect to all degrees of freedom on their free ends. They replicate friction via their elastic-perfectly plastic behaviour. Their yield stress is set to a value that corresponds to the friction force acting on the material. This type of model is appropriate for situations in which the clamping pressure and the tool–prepreg friction coefficient are known.

Material properties for the simulation are based on data and measurements on 3k carbon fibre pre-impregnated fabric in a four by four twill weave manufactured by Hexcel Composites. The matrix was 1947 epoxy resin. The cross-sectional area of the fabric tows was 0.12 mm^2; the shear elements of the model were considered to have the same cross-sectional area. Table 1 summarises the properties used in the finite element model.

Table 1. Material properties used in the model.

Tow modulus (N/mm^2)	S_o(N/mm^2)	S_∞(N/mm^2)	μ	σ
227000	55	2300	0.33	0.02

The shear response of the fabric used in subsequent forming experiments was measured in bias extension tests. The specimen length was 200 mm and its width 70 mm. The strain of a central gauge section within the pure shear zone of the specimen was used to derive a stress-strain curve for the diagonal elements of the unit cell. The speed of the tests (160 mm/min) was similar to the speed of hemisphere forming experiments. It should be noted that the current material model does not take into account viscous effects which would make the material response rate dependent [6]. Also, the tow modulus used does not account for decrimping that can result in a significantly lower apparent modulus at very low strains.

The model was implemented in MSC.Marc (MSC.Software Ltd.). Appropriate user defined subroutines were developed for the incorporation of a non-linear stress-strain response of shear elements, of wrinkling of tow elements and of the elastic-perfectly plastic behaviour of boundary elements.

2.2 Validation of the model

Hemisphere forming experiments were performed to validate the model. Matching hemispheric tools of diameter 60 mm were set on a hydraulic press. Two square clamping plates were used. The upper plate had a 170 mm hole resulting in clamping in the outer region of the fabric. The force acting on the clamping plates was controlled through 4 springs. Forming was performed using clamping forces of 75 N and 133 N. A grid was drawn on the fabric before forming. The spacing of the grid was 10 mm. The positions of all grid points were measured on the formed specimen. Figure 3 shows the formed hemisphere

in the experiment using the high holding force. It can be observed that buckling of tows occurs in the middle of the sides near the base of the hemisphere. The direction of buckling is parallel to the sides of the specimen. It should be noted that a small asymmetry is observed. In order to remove the effects of asymmetry and provide a reliable set of deformation measurements for comparison with the model, an average of the grid positions on the four quarters of the hemisphere was calculated.

The forming of a quarter of the hemisphere was modelled using a truss comprising 312 tow elements, 288 shear elements and 103 friction elements. The total number of nodes modelling the fabric was 169. The size of the unit cell was 10 mm. An additional 103 nodes were used to fix one side of the friction elements. Friction elements remained active while the position of the corresponding node was in contact with both clamping plates. Run times were below 30 sec in all cases.

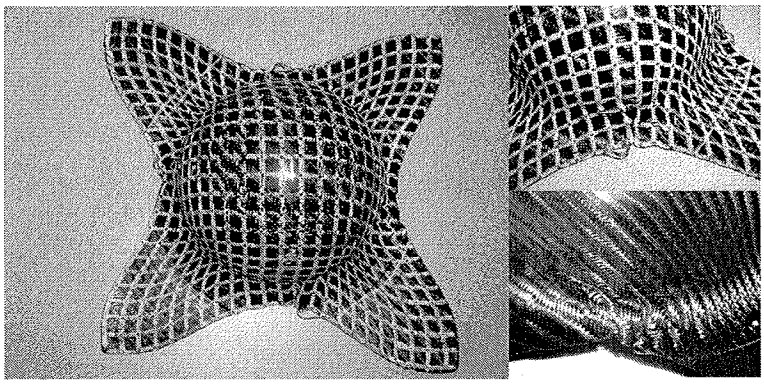

Figure. 3 Formed hemisphere using a holding force of 133 N.

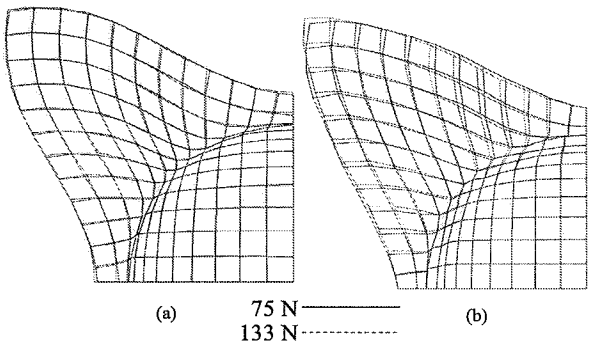

Figure 4. Draped patterns. (a) Experiment. (b) Model.

Figure 4 illustrates the draped patterns measured in experiments and predicted by the model for the two different holding forces. The final shape predicted by the model follows closely the experimental results. Increasing the holding force results in higher shear and lower buckling of tows in both the experiment and model. The sensitivity of shear and wrinkling to the holding force predicted by the model is higher than that observed in the experiments.

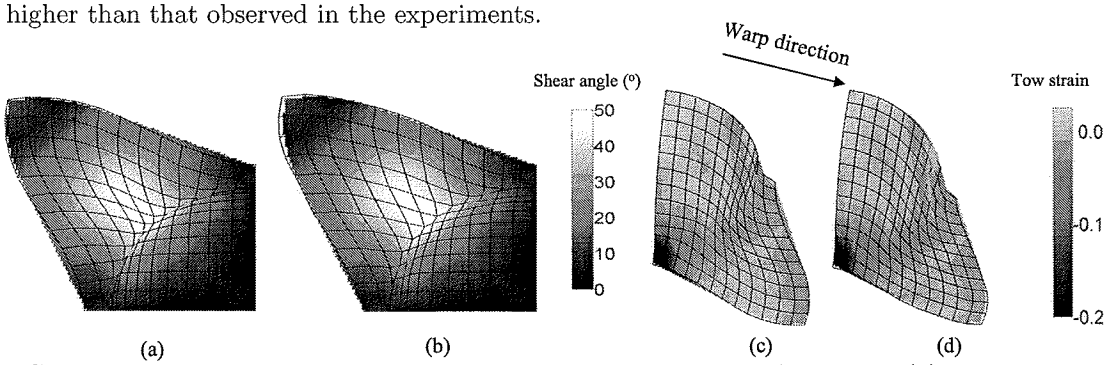

Figure 5. Comparison between experimental and model results in the low force case. (a) Experimental shear pattern. (b) Model shear pattern.(c) Experimental warp tow strain distribution. (d) Model warp tow strain distribution.

The distribution of shear angle over the formed hemisphere for the low holding force case is illustrated in Figures 5.a and 5.b. The shear patterns observed and predicted by the model are very similar. Shear

is maximised, reaching values close to 50°, at the transition from the base to the hemisphere at diagonal positions. Minimum shear occurs at the apex and the middle of the specimen sides.

Figures 5.c and 5.d illustrate the distribution of warp tow strain in the case of low holding force. Wrinkling due to buckling occurs near the base, in the middle of the specimen sides. Compressive strains up to 0.3 are observed. A similar pattern is observed in weft tows due to symmetry. Figures 6.a and 6.b show the shear angle and the wrinkling strain along paths running from the corner of the specimen to the apex and the middle of the specimen side to the apex, respectively. The model replicates the peak observed in the shear angle along the diagonal path. The predicted maximum shear is slightly lower than that measured on the specimen. The magnitude and extent of wrinkling due to tow buckling is reproduced successfully by the model. Tow compression predicted by the model is higher than that measured on the specimen, whereas the wrinkling region predicted is wider.

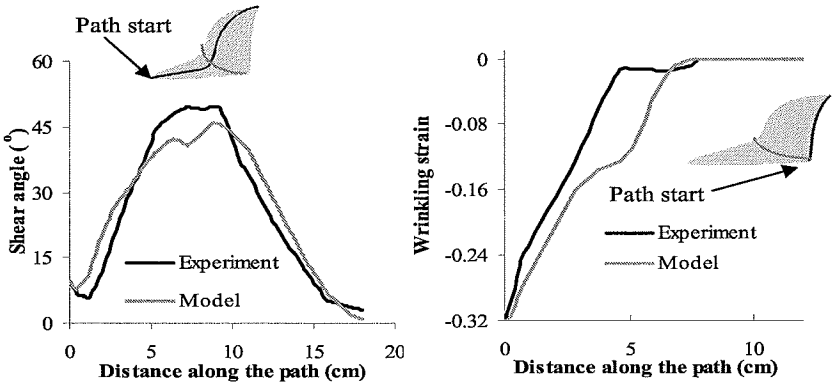

(a) (b)

Figure 6. (a) Shear angle along a diagonal path. (b) Wrinkling strain along a path from the middle of the side to the apex.

3. HOLDING FORCE OPTIMISATION

3.1 Sensitivity of wrinkling strain to holding force

The occurrence of wrinkling which was demonstrated both by experimental and modelling results can be detrimental for the final product quality. For a given part geometry and material, the simplest parameter that can be altered in order to reduce wrinkling is the magnitude and the distribution of the holding force. This can be achieved in practice by changing the tool clamping pressure and its distribution.

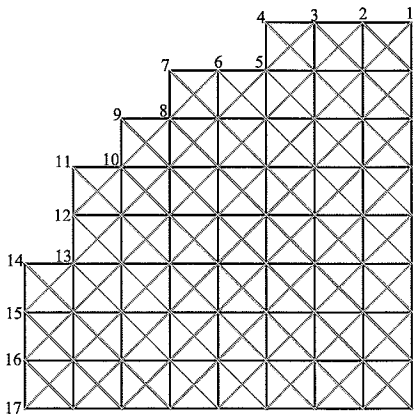

Figure 7. Truss of the hemisphere quarter drape model.

The sensitivity of total wrinkling strain to the holding force was investigated using a model for the forming of a hemisphere with a radius of 40 mm. Friction springs were used only around the perimeter of the fabric, while the initial shape of the fabric was close to circular. Due to symmetry only a quarter of the problem domain was considered. The total number of element was 241, 120 of them were tow elements, 104 were shear elements and 17 were friction elements. The size of the unit cell was 10 mm. The total number of nodes was 86 with 17 of them fixed in all directions. The holding force was applied to the 17 positions numbered in Figure 7.

Figure 8 illustrates the total wrinkling strain, calculated as the sum of wrinkling over all tows of the model, as a function of the holding function applied to each edge node. In this case the same nodal holding force is applied to all nodes. Increasing nodal force results in less wrinkling. The sensitivity of wrinkling strain to the force decreases as force increases.

When uniform clamping is applied wrinkling occurs even at very high forces. It should noted that the clamping forces used in the experiments (75 and 133 N) correspond to nodal forces in the range of 0.4 to 1.2 N. Over this range of forces the total wrinkling strain is between -2.5 and -1.8. Increasing the total clamping force to 1000 N results in total wrinkling strain of about -0.9. It is expected that varying the force profile over the periphery in a suitable manner can decrease total wrinkling without the use of excessive clamping force. The dependence of total wrinkling on the slope of the holding force with respect to angular position was investigated by varying linearly its magnitude from position 1 to 9. The values of the holding force at positions 10 to 17 were considered equal to the values at positions 9 to 1 using the diagonal as a line of symmetry. The force at position 5 was held constant at 0.39 N in all cases. Figure 9 shows the dependence of wrinkling strain on the force differential. It can be observed that applying a higher force at diagonal positions decreases wrinkling by 20%, as a result of higher shear. Similarly, applying a lower force at diagonal positions while increasing the force at normal positions increases wrinkling significantly.

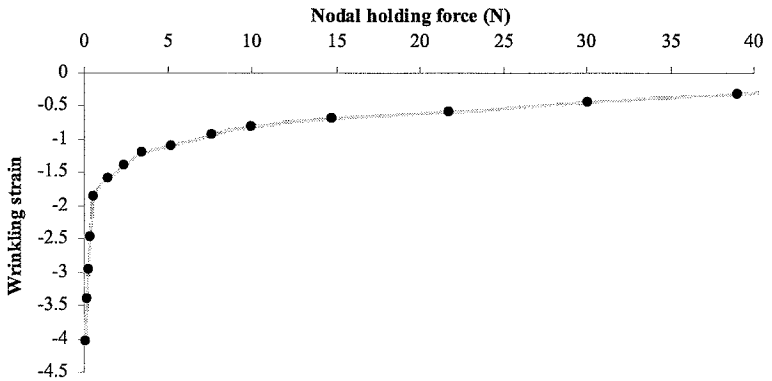

Figure 8. Dependence of total wrinkling strain on the holding force when a constant force is applied over the periphery.

Table 2. Sensitivity coefficients of total wrinkling strain to holding force.

Position	1, 17	2, 16	3, 15	4, 14	5, 13	6, 12	7, 11	8, 10	9
Sensitivity (10^{-2} N^{-1})	2.2	7.3	12.8	6.5	5.5	4.4	11.2	14.1	15.2

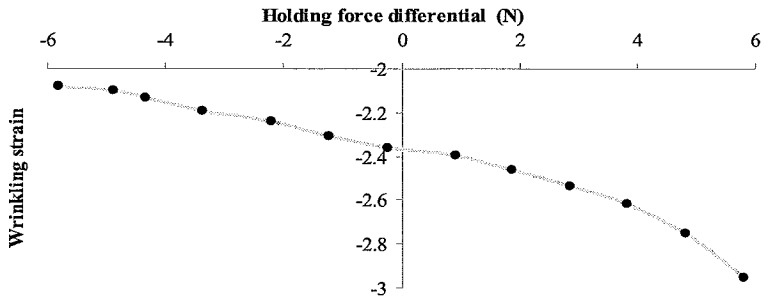

Figure 9. Total wrinkling strain as a function of holding force difference from position 1 to position 9.

The sensitivity of wrinkling strain to nodal holding force was studied by applying a constant holding force profile of 0.39 and increasing the force at each of the positions from 0.39 to 2.39. Table 2 summarises the sensitivity coefficients calculated as the partial derivative of wrinkling strain with respect to nodal holding force. The sensitivity reaches its maximum at the diagonal and its minimum at the normal position. The sensitivity increases rapidly as we move away from the normal position, then decreases to a local minimum value and increases towards the maximum at the diagonal. These results indicate that the highly non-linear character of wrinkling creates a complex relationship between the distribution of holding force and wrinkling strain. In general, increasing the force or the differential between the force at diagonal and normal positions decreases wrinkling. The sensitivity of wrinkling strain to nodal force depends strongly on the position of application.

3.2 Minimisation procedure and regularisation

The objective of optimisation is to minimise wrinkling, i.e. maximise the total wrinkling strain. The objective function can be expressed as follows:

$$W(\mathbf{F}) = \|\varepsilon_{\mathbf{w}}\|_1 \tag{4}$$

where $\mathbf{F}$ is the vector of holding forces, and ε_w is the vector of wrinkling strains of the tow elements with its components defined as follows:

$$\varepsilon_{wi} = \min(0, \varepsilon_i) \tag{5}$$

where ε_i is the strain of element i.

The minimisation is performed using a genetic algorithm. The choice of this type of algorithm instead of a gradient based optimisation technique is dictated by the complex nature of the dependence of wrinkling strain on the nodal holding force applied, as indicated by the sensitivity results presented in the previous paragraph. The genetic algorithm implementation utilised in this study [17] uses binary encoding, elitism, tournament selection, and uniform crossover and mutation operators. The encoding of the problem is performed using nine real valued variables which represent the holding force values at all positions. The real values are represented by four digits resulting in a 36-bit long binary string. This type of encoding was selected instead of real encoding as it allows extension of the optimisation scheme to include discrete variables, such as fabric shape. The range of nodal forces in all runs was 0.3 to 2.5 N. Fifty individuals were used in all cases and the genetic algorithm was run for 40 generations. The mutation probability was 4% and the crossover probability 50%. The number of elite individuals was 7, and the number of individual used in reproduction was 36. The initial population of solutions was generated randomly, the influence of starting population to the final solution was found to be insignificant.

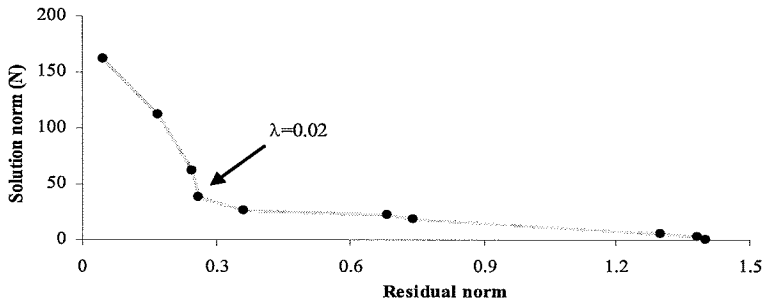

Figure 10. L-curve.

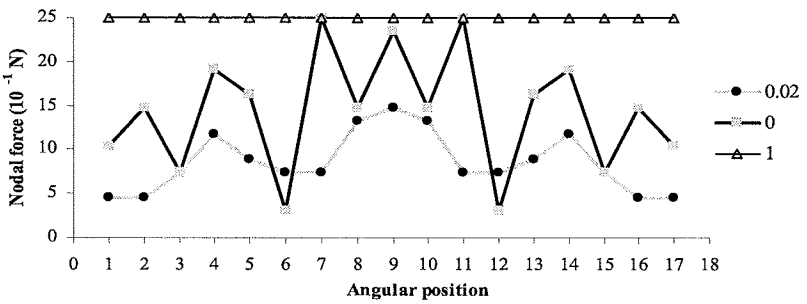

Figure 11. Holding force distribution when different regularisation parameter values are used.

Practical problems faced during composites processing limit the feasibility of some of the potential solutions of the inverse problem. Very high gradients in the holding force might not be achievable in the manufacturing environment. Consequently, the objective is modified with the inclusion of a first order regularisation term as follows:

$$W_\lambda(\mathbf{F}) = \|\varepsilon_{\mathbf{w}}\|_1 + \lambda \|\Delta\mathbf{F}\|_1 \tag{6}$$

Here $\Delta\mathbf{F}$ denotes the force differential and λ is the regularisation parameter. The selection of the regularisation parameter is performed using the L-curve [5]. The optimisation procedure was executed

for values of the regularisation parameter of 0, 5×10^{-3}, 1×10^{-2},2×10^{-2}, 3×10^{-2}, 4×10^{-2}, 5×10^{-2}, 7.5×10^{-2}, 0.2 and 1. The L-curve illustrated in Figure 10 indicates the use of a regularisation parameter equal to 0.02.

The solutions obtained using values of 0, 0.02 and 1 are illustrated in Figure 11. Very high regularisation parameter values result in a flat profile with the total wrinkling strain being equal to -1.4. No regularisation results in negligible wrinkling (approximately -0.05) but a very irregular force profile. When the regularisation parameter is equal to 0.02, wrinkling is kept low (-0.25) while the force profile is relatively smooth. The L-curve indicates the point where wrinkling is kept as low as possible without entering in the regime where further reduction has detrimental effects in terms of force gradients. As suggested in [9] the inclusion of the regularisation term yields results equivalent to those of multi-objective optimisation. In that sense minimisation of the wrinkling strain can be seen as one objective and the force difference norm minimisation as the other.

Figure 12 illustrates the convergence of the genetic algorithm in the case of a regularisation parameter equal to 0.02. The algorithm converges gradually to the final values within 35 generations, which is equivalent to 1750 direct model runs. As the direct model performs a finite element calculation which is highly non-linear with respect to both geometry and material properties (which can be expensive in computational time), the applicability of the inversion procedure depends on the efficiency of the drape model. Therefore the simplified drape model presented here becomes a very useful tool as a part of an optimisation procedure.

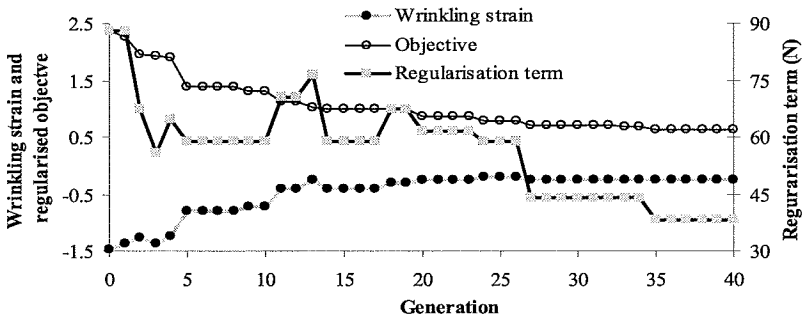

Figure 12. Convergence of the genetic algorithm with regularisation parameter equal to 0.02.

3.3 Optimised drape

The solution obtained using the regularised inverse scheme is compared with a uniform force profile (2.5 N) in Figures 13 and 14.

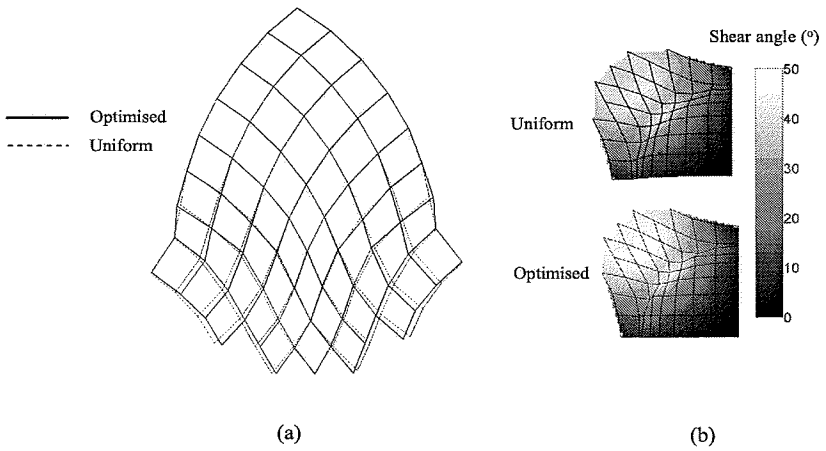

Figure 13. Comparison of optimised and uniform holding force drapes. (a) Draped patterns. (b) Shear angle distributions.

Comparison of the draped patterns (Figure 13.a) and of the distribution of tow strain distributions (Figure 14) shows that the main point of improvement in the optimised drape is the elimination of concentrated buckling at normal positions on the base of the hemisphere. It can also be observed that the shear distribution in the optimised drape is very close to that of the conventional drape (Figure 13.b), with a

slight increase in shear angles on the base in the vicinity of the diagonal being the only difference. As a consequence the initial designs regarding fibre orientation distribution are not affected significantly by the rearrangement of the holding force distribution. This is a consequence of the fact that for most of the component shear angles are governed by changes in curvature.

The distribution of holding force in the optimised solution is illustrated in Figure 14.b. The optimised force distribution achieves minimisation of the wrinkling strain by inducing higher shear at diagonal positions and imposing a high force differential in the areas of concentrated buckling. The implementation of such a design in the manufacturing of composite parts can be performed by varying clamping pressure or by introducing thickness variations in the outer parts of the tools.

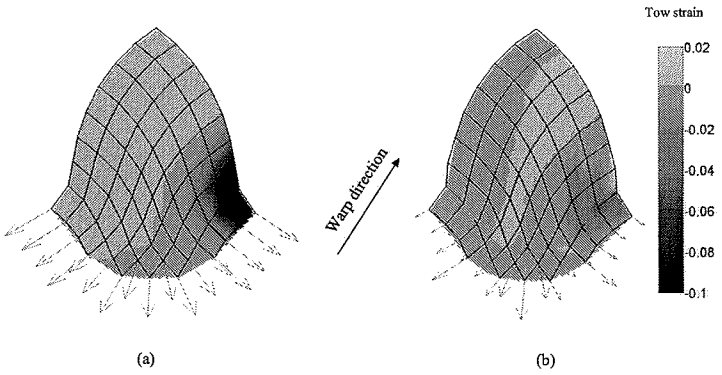

Figure 14. Warp tow strain distribution and holding force distribution. (a) Uniform holding force drape. (b) Optimised drape.

4. CONCLUSIONS

In this paper an optimisation procedure for the draping of woven composites is developed and tested. The procedure is based on the use of an efficient drape model that enables fast solution of the direct model, with the most significant features of the process being reproduced successfully. The performance of the direct model is evaluated against experimental results obtained from the forming of composite hemispheres.

The inverse problem is solved using a binary encoding genetic algorithm with elitism. It is found that regularisation can improve the results of optimisation by imposing a limitation to very high holding force differentials that can affect the feasibility of optimised designs.

The case of hemisphere forming is used to evaluate the performance of the optimisation procedure. The value of the regularisation parameter is determined using the L-curve. The optimised holding force distribution results in the elimination of concentrated buckling of tows at normal positions on the base of the hemisphere. At the same time shear angle distributions are not affected greatly, leaving initial designs concerning fibre orientation unaffected.

Acknowledgement

Contributions from the University of Nottingham, EPSRC, CONACyT, MSC.Software Ltd, DSTL, UK Ministry of Defence, Hexcel Composites, Granta Design Ltd., Ford Motor Company Ltd., Polynorm Plastics (UK) Ltd., Virtual Prototyping Solutions Ltd., Saint-Gobain Vetrotex International SA and ESI Software SA are gratefully acknowledged. The authors are grateful to Dr Phil Harrison of the University of Nottingham for his assistance with the experiments.

REFERENCES

1. S. Bickerton, P. Simacek, S. H. Guglielmi and S. G. Advani, Investigation of draping and its effects on the mold filling process during manufacturing of a compound composite part. *Compos. Part A-Appl. S.* (1997) **28**, 801-816.

2. A. Cherouat and J. B. Billoet, Mechanical and numerical modelling of composite manufacturing processes deep-drawing and laying-up of thin pre-impregnated woven fabrics. *J. Mater. Process Tech.* (2001) **118**, 460-471.

3. L. Dong, C. Lekakou and M. G. Bader, Processing of composites: Simulation of the draping of fabrics with updated material behaviour law. *J. Compos. Mat.* (2001) **35**, 138-163.

4. A. Gokce and S. G. Advani, Simultaneous gate and vent location optimization in liquid composite molding processes. *Compos. Part A-Appl. S.* (2004) **35**, 1419-1432.

5. P. C. Hansen, The use of the L-curve in the regularization of discrete ill-posed problems. *SIAM J. Sci. Comput.* (1993) **14**, 1487-1503.

6. P. Harrison, M. J. Clifford, A. C. Long and C. D. Rudd, A constituent-based predictive approach to modelling the rheology of viscous textile composites. *Compos. Part A-Appl. S.* (2004) **35**, 915-931.

7. P. Harrison, M. J. Clifford and A. C. Long, Shear characterisation of viscous woven textile composites: A comparison between picture frame and bias extension experiments. *Compos. Sci. Technol.* (2004) **64**, 1453-1465.

8. R. Mathur, S. G. Advani and B. K. Fink, A real-coded hybrid genetic algorithm to determine optimal resin injection locations in the resin transfer molding process. *CMES-Comp. Model. Eng.* (2003) **4**, 587-601.

9. N. S. Mera, L. Elliott and D. B. Ingham, A multi-population genetic algorithm approach for solving ill-posed problems. *Comput. Mech.* (2004) **33**, 254-263.

10. D. J. Michaud, A. N. Beris and P .S. Dhurjati, Thick-sectioned RTM composite manufacturing, part II. Robust cure cycle optimization and control. *J. Compos. Mat.* (2002) **36**, 1201-1231.

11. R. K. Miller, J. M. Hedgepeth, V. I. Weingarten, P. Das and S. Kahyai, Finite element analysis of partly wrinkled membranes. *Comput. Struct.* (1985) **20**, 631-639.

12. M. Mitchell, *An Introduction to Genetic Algorithms*, MIT Press, USA, 1998.

13. M. Nguyen, I. Herszberg and R. Paton, The shear properties of woven carbon fabric. *Compos. Struct.* (1999) **47**, 767-779.

14. A. K. Picket, T. Queckborner, P. De Luca and E. Haug, An explicit finite element solution for the forming prediction of continuous fibre-reinforced thermoplastic sheets. *Compos. Manuf.* (1995) **6**, 237-243.

15. P. Potluri, S. Sharma and R. Ramgulan, Comprehensive drape modelling for moulding 3D textile preforms. *Compos. Part A-Appl. S.* (2002) **32**, 1415-1424.

16. S. B. Sharma and M. P. F. Sutcliffe, A simplified finite element model for draping of woven material. *Compos. Part A-Appl. S.* (2004) **35**, 637-643.

17. A. A. Skordos and I. K. Partridge, Inverse heat transfer for optimization and on-line thermal properties estimation in composites curing. *Inverse Probl. Sci. Eng.* (2002) **12**, 157-172.

18. J. Spoerre, C. Zhang, B. Wang and R. Parnas, Integrated product and process design for resin transfer molded parts. *J. Compos. Mat.* (1998) **32**, 1244-1272

19. F. Trochu, A. Hammami and Y. Benoit, Prediction of fibre orientation and net shape definition of complex composite parts. *Compos. Part A-Appl. S.* (1996) **27**, 319-328.

20. F. Van Der Weeen, Algorithms for draping fabrics on doubly curved surfaces. *Int. J. Numer. Meth. Eng.* (1991) **31**, 1415-1426.

21. Q. Zhu and P. H.Geubelle, Dimensional accuracy of thermoset composites: Shape optimization. *J. Compos. Mat.* (2002) **36**, 647-672.